IMEKO 22nd TC3, 12th TC5 and 3rd TC22 International Conferences
3 to 5 February, 2014, Cape Town, Republic of South Africa

DETERMINATION OF PRESSURE TRANSDUCER SENSITIVITY TO HIGH FREQUENCY VIBRATION

S. Downes, A. Knott, and I. Robinson

National Physical Laboratory (NPL), Hampton Road, Teddington, United Kingdom, TW11 0LW

Abstract: This paper reports on an investigation into the sensitivity of one type of piezoelectric pressure transducer to the acceleration of its support mount, when located in the end wall of a shock tube and subjected to a very fast pressure step. Support mounts of different materials are used, together with laser vibrometry measurements of the back face of the mount, in an attempt to separate the part of the signal due to the acceleration from that due to the pressure step.

Keywords: Laser vibrometry, pressure, transducer, acceleration, sensitivity, shock tube

1. INTRODUCTION

The accurate measurement of pressure is critical in a wide range of industrial applications. In many of these applications, such as combustion engine development, the pressure is changing rapidly, but suitable dynamic calibration facilities for the pressure sensors do not exist [1]. As part of a European project (EMRP IND09) to establish traceable dynamic calibration facilities for force, torque, and pressure measurement systems, NPL has developed a 1.4 MPa shock tube (Figure 1) capable of generating, and then applying to the pressure transducer diaphragm, an extremely rapid pressure step (theoretical calculations predict rise times of the order of a nanosecond).

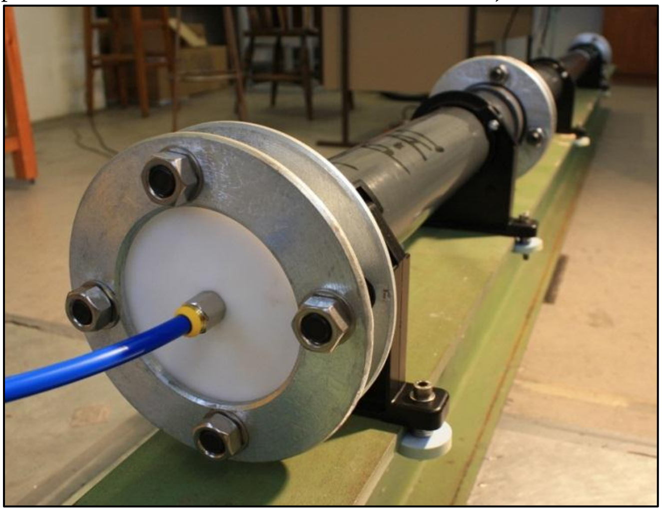

Figure 1: NPL 1.4 MPa shock tube, viewed from driver end

The output of the pressure measurement system after arrival of the shock front is a combination of its response to the step pressure change and its response to the acceleration induced by the vibration of its support mount, which has been excited by the same shock front.

The work described attempts to separate these two influences, to enable the transducer's response to a pressure step alone to be determined.

2. PRESSURE MEASUREMENT SYSTEM

The piezoelectric pressure sensor being characterised in this work is a Kistler 603B 20 MPa device, attached to a Kistler 5015A charge amplifier, whose output voltage is recorded at a rate of 2 MHz by a National Instruments PXI-5922 flexible resolution digitizer. A bespoke LabVIEW program controls the data acquisition and subsequent analysis.

Kistler states that the sensor's acceleration sensitivity is <0.01 kPa/g, that its natural frequency is ≈400 kHz, and that the charge amplifier has an analogue low pass filter of 200 kHz.

3. SHOCK TUBE ARRANGEMENT

Figure 2 illustrates the sensor mount itself – the transducer's diaphragm is set flush to the mount's flat face – while Figure 3 demonstrates how the mount is located within the tube.

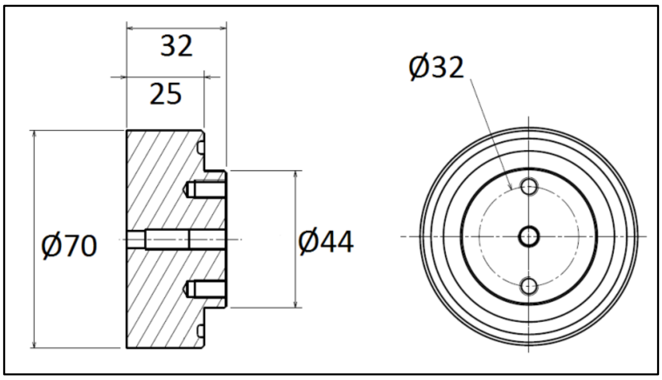

Figure 2: Sensor mount, dimensions in mm

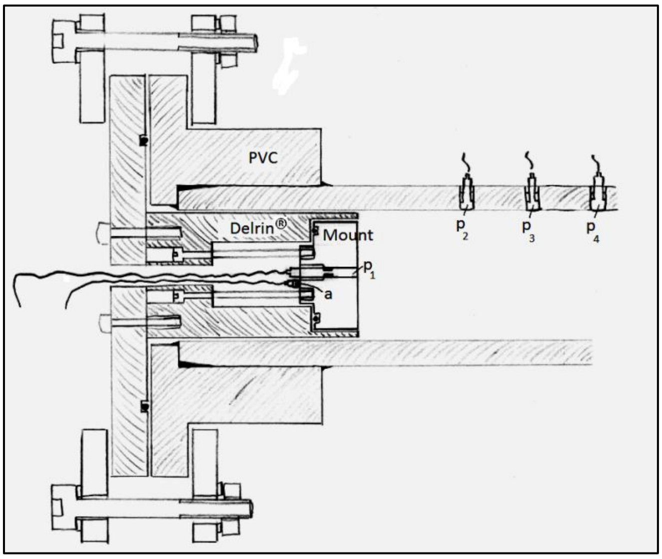

Figure 3: Tube end arrangement

The shock front is initiated by increasing the pressure in the driver end of the shock tube until a brass diaphragm separating it from the driven end ruptures [2]. The magnitude of the shock front pressure step, for diaphragm material of the same thickness, is repeatable to within a few percent and can be calculated using measurements of the shock front velocity. For a 0.1 mm thick diaphragm, reflected pressure steps of approximately 0.8 MPa are created at the end wall of the tube. The structure of the waveform recorded by the pressure transducer mounted in the end wall is extremely repeatable for a given set of experimental conditions, as shown in Figure 4, in which the waveforms recorded during three successive shock tube firings using 0.1 mm diaphragms are shown.

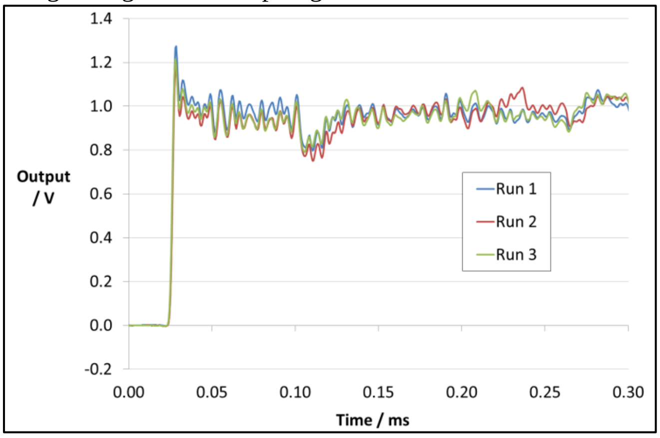

Figure 4: Repeatability of transducer waveforms

In an attempt to separate that part of the waveform resulting from the transducer's dynamic response to the step pressure change from that part caused by its sensitivity to the vibration of its steel mount (excited by the same pressure event), sensor mounts of identical geometry were manufactured from three other materials: aluminium, brass, and Delrin®, a machinable thermoplastic (polyoxymethylene). The transducer was then held in each of these mounts, in turn, and subjected to three shock excitations generated within the tube, two from 0.1 mm diaphragms and the final one from a 0.05 mm diaphragm. This change of sensor mount material resulted in significantly different waveforms, as shown in Figure 5, where the traces resulting from the initial 0.1 mm diaphragm tests for the four materials are shown.

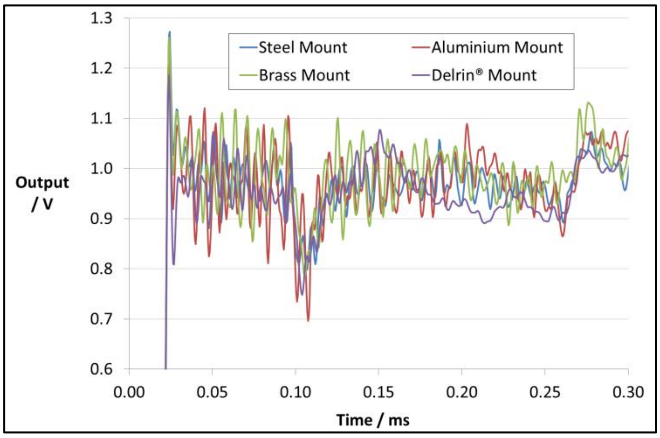

Figure 5: Output traces for different sensor mount materials

Although the underlying characteristics for each of the four traces seem similar, there are differences in both the amplitude and frequency of the variations about this underlying trend. A simple FFT analysis of these traces, based on the 2048 data points (an interval of just over 1.0 ms) after the initial peak value, is given in Figure 6 and clearly illustrates these differences.

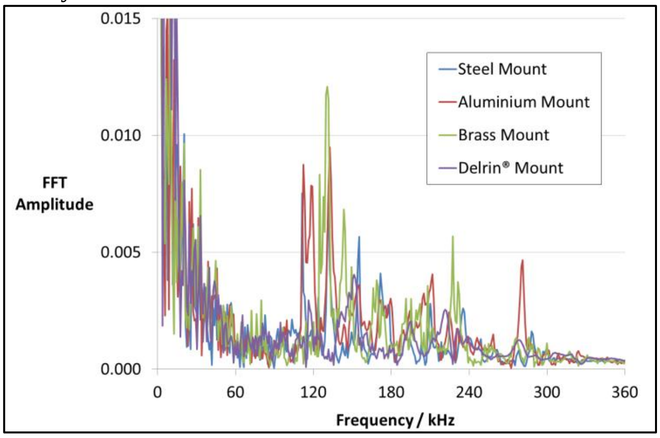

Figure 6: FFT plots for different sensor mount materials

Table 1 details the elastic properties of the materials used for the four blocks and gives the calculated speed of longitudinal sound waves within each. These speeds should be proportional to the resonant frequencies of the blocks – the faster sound waves propagate through them, the higher their "ringing" frequency should be.

Table 1: Sensor mount material data

Material	Elastic modulus E / GPa	Density ρ / kg·m^{-3}	Poisson's ratio ν	Speed of sound c / m·s^{-1}
Steel	210	7 800	0.295	5 980
Aluminium	70	2 700	0.345	6 380
Brass	101	8 500	0.350	4 370
Delrin®	3	1 420	0.350	1 840

In order to determine which part of the FFT frequency content might be due to the transducer's sensitivity to vibration, and which part was therefore due to the transducer's response to a dynamic pressure step, a direct measurement of the movement of the sensor mount was necessary. Initial tests were performed with an accelerometer adhered to the rear surface of the steel sensor block, but the relatively low frequency response of the device prevented any useful measurements being made. An alternative approach of using a laser vibrometer was therefore adopted.

4. LASER VIBROMETRY

A Polytec PSV-400-M2-20 scanning vibrometer, an instrument based on the Doppler-effect and capable of measuring the velocity of surfaces at working distances from 80 mm to 100 m at frequencies of up to 10 MHz, was used to make the required vibration measurements. The vibrometer was used in its velocity mode with a sensitivity of 1 $V\cdot(m\cdot s^{-1})^{-1}$ and a data acquisition rate of 2.56 MHz.

For each of the four sensor mounts, the pressure transducer was fitted and then subjected within the shock tube to nominally-identical pressure steps, with the vibrometer recording the motion of a location on the rear face of the sensor mount. The vibrometer data acquisition system was set up to have the same pre-trigger period as the pressure transducer data acquisition system and to be triggered simultaneously using the output from the pressure transducer. As well as being digitally recorded by the vibrometer system, an analogue output from the vibrometer was also recorded synchronously by the pressure transducer's data acquisition system, to simplify the subsequent data analysis procedure.

5. RESULTS

As an example, part of the recorded velocity waveform from one of the tests with the aluminium mount is shown in Figure 7. The shockwave arrives at approximately 10.23 ms – the changing velocity prior to this is caused by the tensile stress wave in the tube wall, which travels faster than the shock front, accelerating the end mount back towards the tube's driver section.

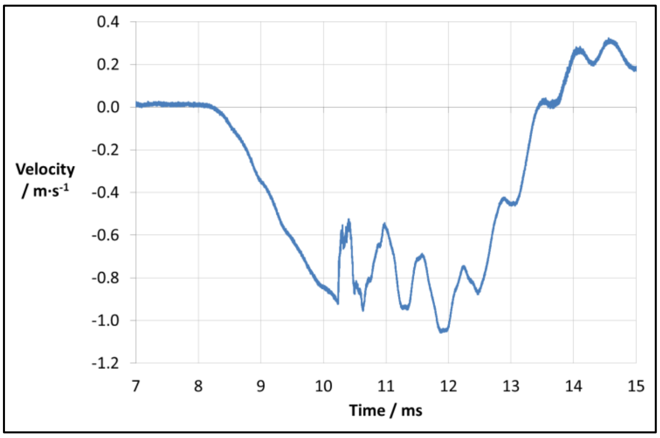

Figure 7: Velocity waveform from aluminium mount

When analysing the recorded data, the first question to be answered was whether or not the analogue vibrometer signal recorded by the pressure transducer data acquisition system was a reliable representation of the digital value recorded by the vibrometer system. Figure 8 compares the outputs from the two systems during a 0.15 ms period which includes the arrival of the shock front. The frequency content of these two traces, over a period of 2048 samples (0.800 ms for the vibrometer instrumentation and 1.024 ms for the pressure transducer acquisition kit) from a time of 10.0 ms is shown in Figure 9. Taken together, these figures demonstrate that the analogue output is a reasonably faithful reproduction of the digital waveform, with possibly less high frequency noise – all subsequent analysis was therefore performed using the vibrometer data recorded by the PXI-5922 digitizer.

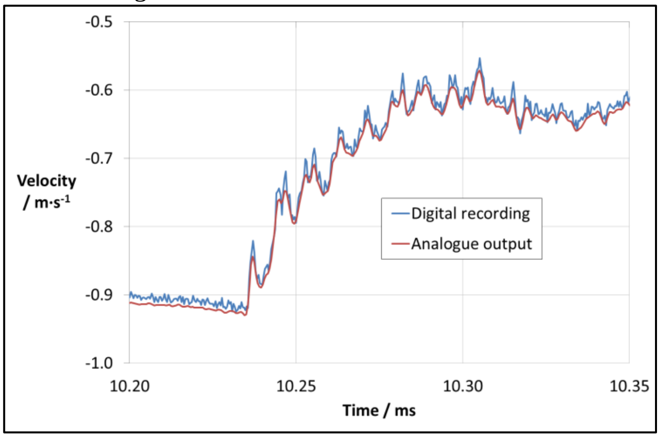

Figure 8: Aluminium sensor mount velocity waveforms

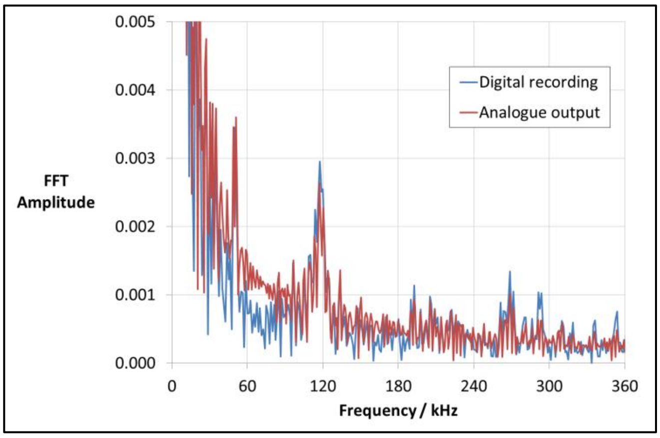

Figure 9: Frequency content of velocity waveforms

The velocity waveforms were converted into acceleration waveforms by simple digital processing, taking the difference between the two velocity values either side of each sample time and dividing this difference by the period separating the velocity values, i.e. 1 µs. Figures 10 and 11 show the acceleration plots resulting from the velocity waveform given in Figures 7 and 8.

According to the Kistler data sheet, the maximum recorded acceleration of 57 600 $m\cdot s^{-2}$ should affect the sensor output by less than 59 kPa, equivalent to 0.073 V in Figure 5.

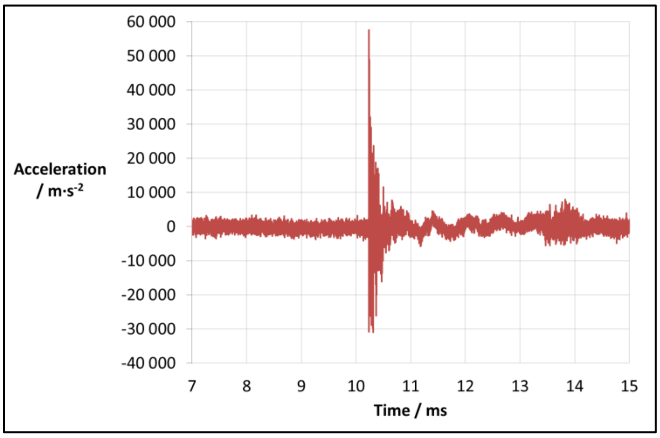

Figure 10: Acceleration waveform from aluminium mount

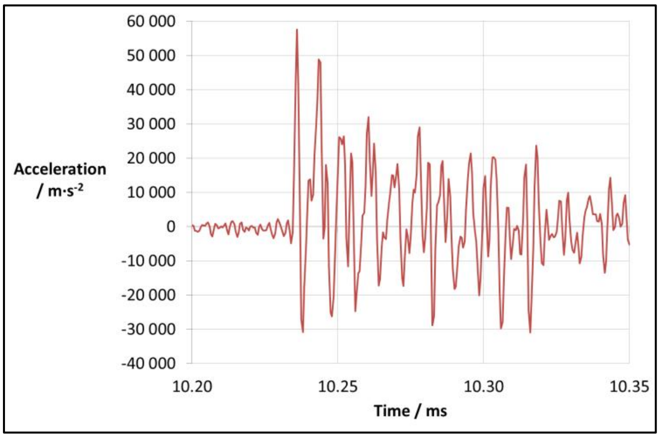

Figure 11: Acceleration waveform from aluminium mount

The frequency content of this acceleration waveform for the 1.024 ms period starting at 10 ms is given in the FFT amplitude plot, shown in Figure 12. As expected, the frequencies at which peaks occur are similar to those for the velocity signal, as shown in Figure 9.

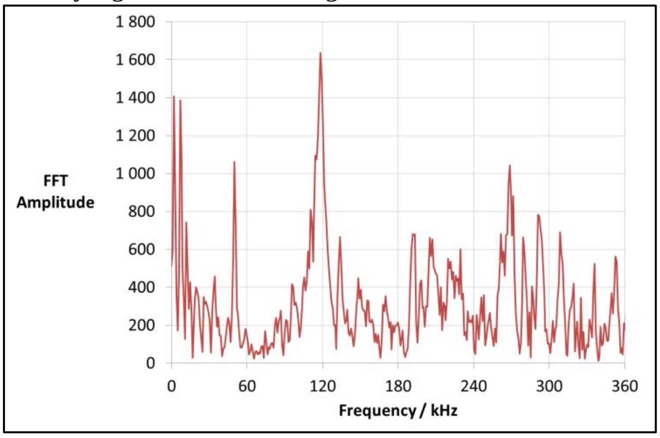

Figure 12: Frequency content of acceleration waveform

The frequency content resulting from the repeat measurement using the aluminium block was virtually identical, and the content using a smaller pressure step (obtained from a diaphragm of 0.05 mm rather than 0.1 mm) displayed peaks at the same frequency values, albeit with lower amplitudes. This repeatability was also evident for all other block materials so, for clarity, only one waveform for each material is considered from this point forwards. In each case, this is the waveform obtained from the test using the 0.05 mm diaphragm. Figure 13 plots the frequency content obtained from the four different block materials, showing the effect of the material's mechanical and elastic properties on the block's vibration.

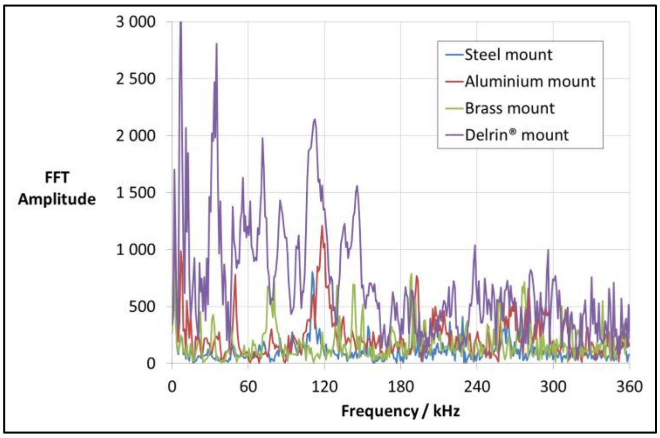

Figure 13: Acceleration frequency content

The frequencies of 35 kHz for Delrin®, 80 kHz for brass, 110 kHz for steel, and 118 kHz for aluminium, at which peak amplitudes occur, are directly proportional to the speed of sound in the material, giving a wavelength of approximately 54 mm. This is a reasonable value when considering that, during a single vibration cycle, the elastic wave will be travelling a distance of twice the thickness of the block, a thickness which varies from 25 mm to 32 mm.

Figures 14 to 17 compare, for each sensor mount material, the frequency content of the block's acceleration and the frequency content of the pressure transducer output.

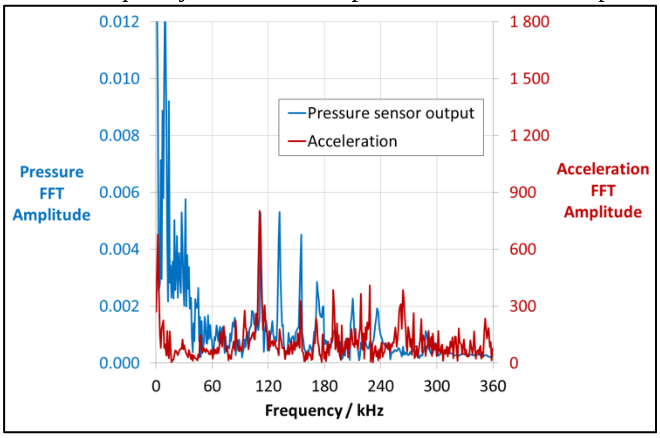

Figure 14: Steel sensor mount performance

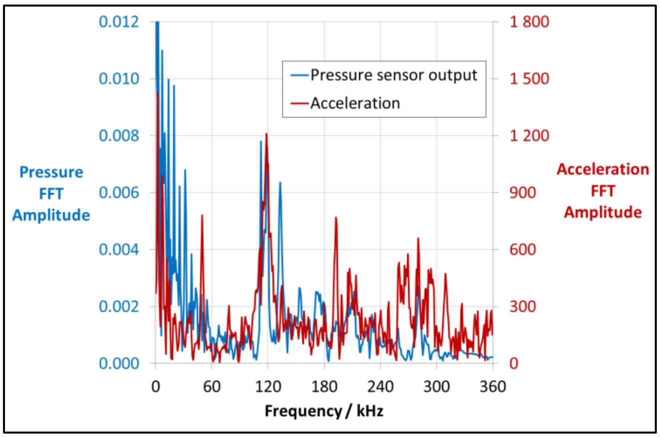

Figure 15: Aluminium sensor mount performance

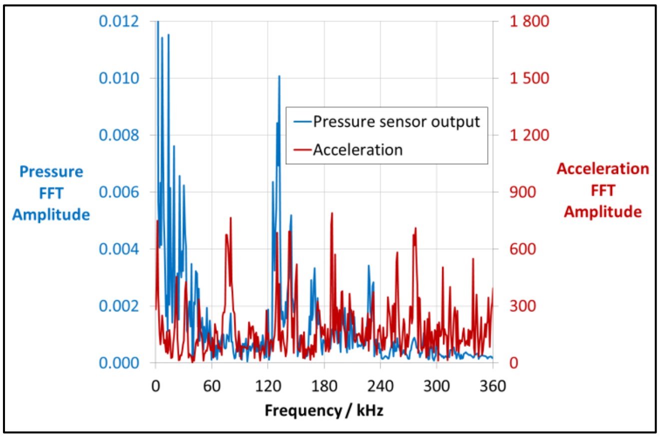

Figure 16: Brass sensor mount performance

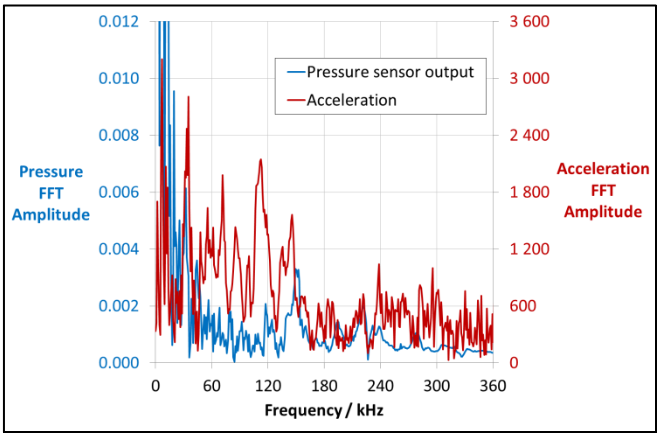

Figure 17: Delrin® sensor mount performance

It is apparent from these figures that, for the three metallic materials, there are peaks in the pressure sensor output corresponding to the peak frequencies identified in Figure 13, suggesting that the sensor is sensitive to vibrations along its axis – this effect is less pronounced for the brass mount, possibly because the sensor's in-built acceleration compensation performs better at this lower frequency level.

In addition, there are other frequencies at which there are peaks in the pressure sensor output, some of which correspond to other acceleration peaks and some which do not; there are also acceleration peaks which do not appear to excite vibration in the pressure sensor.

For the Delrin® sensor mount, the results are somewhat different. Despite significantly higher levels of acceleration, the pressure sensor output appears less sensitive to it, with no sharp peaks at specific frequencies. This is likely to be due to the plastic nature of the material both spreading the energy more uniformly across the frequency range and being less able to couple the acceleration into the sensor. It may also damp out some of the vibration inherent in the sensor.

To try to identify those frequencies at which an increase in pressure sensor output cannot be explained by its axial acceleration sensitivity, Figure 18 plots, for each material, the ratio of the pressure sensor frequency dependence to the frequency content of the acceleration. Each metallic material displays a peak ratio at approximately 131 kHz, strongly suggesting that there is a material-independent effect at this frequency, likely to be due to the dynamic characteristics of the pressure sensor itself.

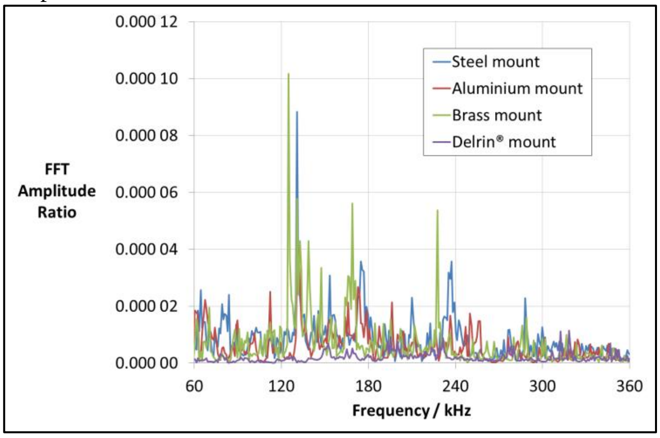

Figure 18: Frequency effects not due to acceleration

Again, for Delrin®, these effects are not present, suggesting that the nature of the material has helped to damp out such vibrations within the sensor.

6. CONCLUSIONS

The following conclusions can be drawn from the results obtained:

- When the pressure sensor is mounted directly in a metallic holder, its output has a frequency component corresponding to the holder's primary mode of longitudinal vibration, particularly for frequencies above 100 kHz. This suggests that the sensor is sensitive to longitudinal accelerations in this frequency range.
- The sensor's output frequency characteristic varies between the different metallic holders and is quite complex – in addition to the frequency of the holder's primary mode of longitudinal vibration, there are a number of further frequency peaks, some of which are correlated with the holder's vibration and some of which are not. Those which are not may be due to the sensor's inherent dynamic characteristics, or they may be the result of sensitivity to transverse vibrations which would be undetected by the vibrometer. Future

work could investigate lateral movement of the holder to determine whether or not such vibrations are present.

- Notwithstanding the previous point, a frequency of approximately 131 kHz was identified, at which there was a strong sensor output frequency peak for all three metallic holder materials, with little longitudinal acceleration. It is likely that this is a fundamental characteristic of the sensor's dynamic performance.
- Despite higher levels of acceleration, tests using the Delrin® holder resulted in significantly less high-frequency "ringing" of the sensor output, presumably due to the plastic nature of the material not enabling distinct vibration frequencies to be initiated and even damping out any inherent sensor vibration. A combination of the high-frequency filtering characteristics of plastic and the stiffness and inertia of steel may therefore present an optimal mounting solution for this sensor type. In industrial applications where high-frequency vibrations are present, plastic mounting adaptors are commonly used – they were not employed during this research as the aim was to characterise the transducer response to acceleration, but their use in practical applications can deliver significant benefits.

7. REFERENCES

[1] T. J. Esward, C. Elster, J. P. Hessling, "Analysis of Dynamic Measurements: New Challenges Require New Solutions," IMEKO XIX World Congress, Lisbon, 2009.

[2] D. W. Holder and D. L. Schultz, "On the Flow in a Reflected-Shock Tunnel," HMSO, London, 1962.

The authors gratefully acknowledge support and funding for this work from the National Measurement Office (under the UK National Measurement System Engineering & Flow Metrology Programme). The EMRP is jointly funded by the EMRP participating countries within EURAMET and the European Union.

© Queen's Printer and Controller of HMSO, 2014